

Scaling properties of InAs/GaAs self-assembled quantum dots

Y. Ebiko, S. Muto, D. Suzuki, S. Itoh, H. Yamakoshi, K. Shiramine, and T. Haga
Department of Applied Physics, Hokkaido University, N13 W8 Kitaku, Sapporo 060-8628, Japan

K. Unno and M. Ikeda

Division of Electronic and Information Engineering, Hokkaido University, N13 W8 Kitaku, Sapporo 060-8628, Japan

(Received 21 April 1999)

We studied the scaling law for volume distribution of the self-assembled quantum dots grown by molecular-beam epitaxy of the Stranski-Krastanow mode. The scaling law was found to hold regardless of the annealing time and growth temperature. Also, we found the scaling law for the pair distribution of self-assembled quantum dots. Both the volume distribution and pair distribution agreed with the scaling functions for two-dimensional submonolayer homoepitaxy model with critical cluster size $i = 1$, which excludes adatom detachment from clusters. [S0163-1829(99)04835-3]

I. INTRODUCTION

Recently much attention has been paid to the growth mechanism of dislocation-free self-assembled quantum dots by the Stranski-Krastanow (SK) mode, because the self-assembled quantum dot is a structure with high potentiality for laser and memory applications. However, the current quantum dots have volume fluctuation which is commonly $\pm 10\%$ too large for the laser application. In this paper we discuss the scaling properties of the distributions of the molecular-beam epitaxy (MBE) grown InAs/GaAs SK quantum dots.

In the case of submonolayer epitaxial growth, the island volume scaling is well studied by means of the scanning tunneling microscope (STM) observations¹⁻⁴ and computer simulations.⁶⁻⁸ According to the scaling assumption^{9,10} the island volume (more precisely, the island area, in this case) distribution is described by

$$N_s = \frac{\langle s \rangle^2}{\Theta} f\left(\frac{s}{\langle s \rangle}\right). \quad (1)$$

Here N_s is the density of the islands which contain s atoms, Θ is the fractional surface coverage, $\langle s \rangle$ is the average number of atoms in an island, and $f(s/\langle s \rangle)$ is the island volume distribution scaling function. The volume distribution scaling law (1) is well known to hold for two-dimensional islands of homo and hetero submonolayer epitaxy, such as Fe on Fe (Ref. 1) and InAs on GaAs (Ref. 2) and also for their growth simulations.

II. EXPERIMENT

The growth was done by the Riber 2300 molecular-beam epitaxy system on nominally flat GaAs (001) substrate. After the growth of the GaAs buffer layer at a substrate temperature of 600 °C, we decreased the temperature to 490 °C, the surface reconstruction is $c(2 \times 4)$, and the InAs was grown (at a rate of 0.1 $\mu\text{m/h}$ with arsenic pressure of 5×10^{-6} Torr). We prepared two types of samples at 490 °C. One was obtained by 60-s annealing, that is 490 °C, 60-s annealing

under As pressure after the InAs growth. The other was obtained without annealing, that is, immediately cooled down after the In shutter was closed. Furthermore, we varied the growth temperature, for samples from 510 °C to 560 °C without annealing. The substrate rotation was stopped during the InAs growth to obtain different coverages within a single growth run and to observe the reflection high-energy electron diffraction pattern. The substrates were taken out of the MBE chamber after they cooled down to room temperature. The islands were characterized by atmospheric atomic force microscopy (Nano Scope III) after the epiwafer was taken out of the MBE chamber. As for 60-s annealing, we have already reported the presence of the volume distribution scaling function.¹¹

III. RESULT

Figures 1(a) and 1(b) show the average InAs dot volume for various dot density. Here, we defined dot volume by the product [(110) diameter] \times [$\bar{1}10$ diameter] \times [height]. In fact, for a cone-shape dot, the volume is $\frac{1}{3}$ of height \times base area, and for a cap-shaped dot the prefactor is $\frac{1}{2}$. However, we note that the scaling function is independent of the prefactor of the volume.

As we increased the growth temperature, the dot size simply increased. However, at 550 °C we observed a different feature on the surface: there are two types of dots. One type is of large dots, whose diameter is about 50 nm and height is 5.5 nm, the other type is of small dots (diameter: 20 nm, height: 1.5 nm). We also observed a holelike structure whose depth is 1~2 ML. Finally at 560 °C, there are only large scale three-dimensional (3D) structures, and quantum-size dots vanished.

In Fig. 1(a), for samples of 490 °C with a dot density more than $3 \times 10^{10}/\text{cm}^2$, the average dot volume decreased as the dot density increased. We attribute this tendency to the increased probability of dot nucleation. It was reported¹⁷ that the total dot density ρ showed the power law as a function of the coverage expressed as

$$\rho = \rho_0 (\Theta - \Theta_c)^\alpha, \quad (2)$$

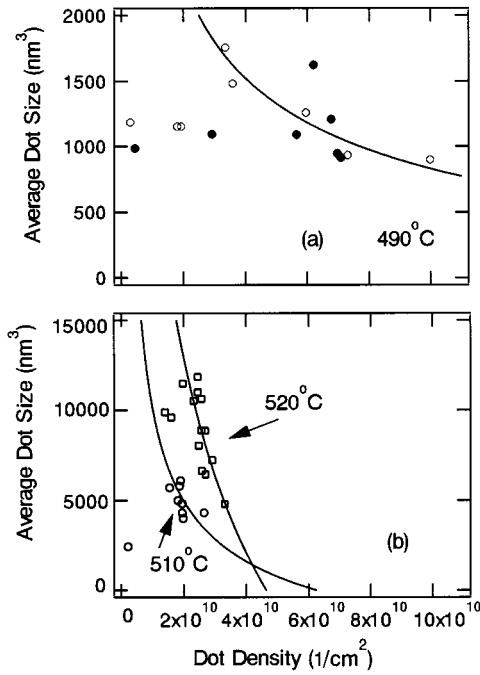


FIG. 1. (a) Average dot volume as a function of dot density at growth temperature 490 °C. The open circle was obtained from the sample with 60-s annealing. The solid circle was obtained from the sample without annealing. (b) The average dot volume as a function of dot density at 510 °C (○), 520 °C (□). The solid curves are eye guides.

where ρ_0 is a proportionally coefficient, Θ_c is the critical coverage (1.5 ML), and the critical exponent α was 1.76 at 490 °C.¹⁷ Since dot nucleation is proportional to $(\Theta - \Theta_c)^{1.76}$, and increases more rapidly than the In supply increase as $(\Theta - \Theta_c)$, each dot catches less In adatoms as we increase coverage. In short, the In supply for each dot decreases as we increase the coverage, and so the average of the dot volume decreases.

For dot density less than $3 \times 10^{10}/\text{cm}^2$, we could observe a quasi-3D island⁵ and a 2D island on the substrate. As long as there was a quasi-3D island, the island volume was smaller. Here we believe that diffusing In adatoms could not arrive at existing dots because of low dot density. The same interpretation is applied to the sample with higher growth temperature. For example, at 510 °C, with a density more than $2.0 \times 10^{10}/\text{cm}^2$, the average dot volume decreased as the dot density increased. Also in this sample we could observe quasi-3D islands at a density less than $2.0 \times 10^{10}/\text{cm}^2$, where dot volumes are small. It suggests that the adsorption of diffusing In adatoms, probably to 2D step edges, without reaching dots leads to the nucleation of a quasi-3D island. In addition, from Eq. (2), the average dot volume $\langle s \rangle$ is described by $\langle s \rangle \sim \rho^{1/\alpha - 1}$. Therefore, Fig. 1 implies that the growth temperature increased the critical exponent α .

Figure 2 shows the volume distribution of InAs quantum dots with 60-s annealing. At low dot density, the volume distribution is broad, and the volume fluctuation is large. At high density, the volume distribution sharpens: volume fluctuation is small and large dots observed at low density do not exist. This trend is opposite from the 2D homoepitaxy in the scaling region,⁷ in which there is no nucleation of a new island, and 2D islands became larger as the coverage in-

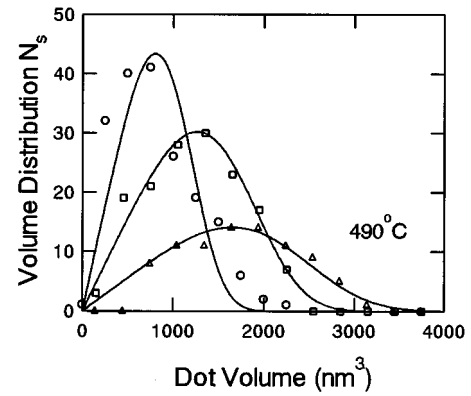


FIG. 2. Volume distribution of the sample with 60-s annealing at 490 °C. Dot density is $3.36 \times 10^{10}/\text{cm}^2$ (Δ), $5.96 \times 10^{10}/\text{cm}^2$ (\square), $7.32 \times 10^{10}/\text{cm}^2$ (\circ). The solid curves are eye guides.

creased. However, in the case of a self-assembled quantum dot, dot nucleation is proportional to $(\Theta - \Theta_c)^\alpha$. Therefore, the dot volume decreased, as we increased coverage.

Figure 3(a) shows island volume scaling functions of samples with and without annealing at 490 °C. Here, the coverage Θ in Eq. (1) was replaced by the effective coverage $\Theta_{eff} = \sum s N_s$ obtained by the total dot volume. Figure 3(b) shows the scaling function at higher temperature. The scaling law was confirmed regardless of annealing times and growth temperature. From Figs. 2, 3(a), and 3(b), we see that the normalized dot volume fluctuation is always constant. The scaling function of Figs. 3(a) and 3(b) also tells us that the growth mechanism did not change, even if the coverage or growth temperature was changed. For the heteroepitaxial system a potential barrier, originated from the lattice mismatch, is said to be formed at the dot edge where strain energy is maximum.¹² This barrier reduces the growth rate for large volume dots. If the potential barrier worked effectively, the scaling function should have depended on the average dot volume because large dots could not grow more. We suppose that the potential barrier did not play an important role for the coverages and temperatures we observed. In Fig. 3(c) of 550 °C, whose surface structure is different from lower temperature, the scaling is also quite different from Figs. 3(a) and 3(b).

In Fig. 3 the solid curves are the scaling function of the homoepitaxial growth simulation model with critical cluster size $i=1$.¹³ In this model a monomer can diffuse on the surface but when it encounters another monomer or a cluster, it stops and forms a stable cluster and there is no more diffusion or detachment. A monomer stops even if only one of its nearest-neighbor sites is occupied in this model. The dashed curve is the scaling function of a model with critical cluster size $i=2$, which has a probability of monomer detachment from a cluster once formed if only one of its nearest-neighbor sites is occupied. The scaling function of the InAs/GaAs self-assembled quantum dot agreed with the model with critical cluster size $i=1$. This scaling function of the growth model with critical cluster size $i=1$ agreed with the low-temperature homoepitaxial Fe on Fe experiment. To our surprise, the scaling function of the quantum dot agreed with the scaling function of submonolayer homoepitaxy [Fe on Fe (Ref. 1)] but disagreed with submonolayer heteroepi-

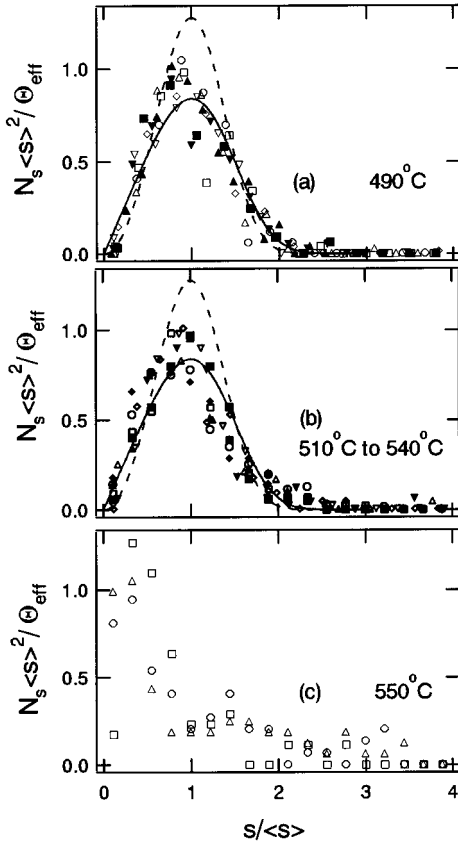


FIG. 3. Volume distribution scaling function at 490 °C (a). Dot densities with annealing are $0.3 \times 10^{10}/\text{cm}^2$ (\circ), $1.8 \times 10^{10}/\text{cm}^2$ (\square), $7.32 \times 10^{10}/\text{cm}^2$ (∇), $10.00 \times 10^{10}/\text{cm}^2$ (\diamond), and without annealing $2.6 \times 10^{10}/\text{cm}^2$ (\blacktriangledown), $4.32 \times 10^{10}/\text{cm}^2$ (\blacksquare), $6.76 \times 10^{10}/\text{cm}^2$ (\triangle), $7.08 \times 10^{10}/\text{cm}^2$ (\blacktriangle). In (b) dot densities are $2.56 \times 10^{10}/\text{cm}^2$ (∇), $2.8 \times 10^{10}/\text{cm}^2$ (\diamond) at 510 °C, $1.96 \times 10^{10}/\text{cm}^2$ (\blacktriangledown), $2.66 \times 10^{10}/\text{cm}^2$ (\blacktriangle) at 520 °C, $1.97 \times 10^{10}/\text{cm}^2$ (\square), $2.68 \times 10^{10}/\text{cm}^2$ (\triangle), $3.31 \times 10^{10}/\text{cm}^2$ (\circ) at 530 °C, $2.54 \times 10^{10}/\text{cm}^2$ (\blacklozenge), $3.16 \times 10^{10}/\text{cm}^2$ (\blacksquare) at 540 °C. In (c), dot densities are $2.55 \times 10^{10}/\text{cm}^2$ (\circ), $2.73 \times 10^{10}/\text{cm}^2$ (\triangle), $2.78 \times 10^{10}/\text{cm}^2$ (\square) at 550 °C. The solid curve is the scaling function of the simulation model with critical cluster size $i = 1$.

taxy [InAs on GaAs (Ref. 2)]. Therefore, the strain coming from the lattice mismatch did not modify the scaling function of our SK dots.

In the case of the 2D homoepitaxial Fe on Fe experiment, since the Arrhenius law control detachment, higher temperatures modified the scaling function. However, in the case of the self-assembled quantum dot, the scaling function did not change up to 540 °C. When we increased the growth temperature to 550 °C the scaling function was quite different from the one for the simulation model with critical cluster size $i = 1-3$. Therefore, a growth mechanism, possibly the desorption, must have worked at 550 °C, in addition to diffusion, aggregation, and detachment.

In Figs. 3(a) and 3(b) the scaling function was unchanged. We can conclude that the same growth mechanism is working regardless of the anneal procedure and growth temperature. However, it should be noted that immediate cooling does not precisely mean 0-s annealing time. There is a 5–10-s delay before the wafer is sufficiently cool, and there is a report based on the photoluminescence study that 10 s is enough to saturate the effect of annealing.¹⁴

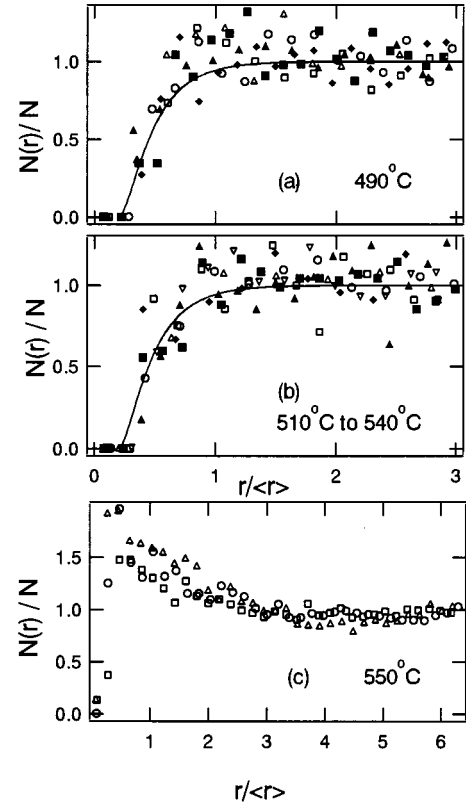


FIG. 4. Pair distribution scaling function. (a) compares the results of 490 °C with and without 60-s annealing. The dot densities with annealing are $3.36 \times 10^{10}/\text{cm}^2$ (\triangle), $7.16 \times 10^{10}/\text{cm}^2$ (\circ), $10.00 \times 10^{10}/\text{cm}^2$ (∇), and without annealing $4.74 \times 10^{10}/\text{cm}^2$ (\blacktriangle), $5.54 \times 10^{10}/\text{cm}^2$ (\blacksquare), $7.15 \times 10^{10}/\text{cm}^2$ (\blacklozenge). In (b) all are obtained without annealing. Dot densities are $2.09 \times 10^{10}/\text{cm}^2$ (\blacklozenge), $2.81 \times 10^{10}/\text{cm}^2$ (\blacksquare) at 510 °C, $2.85 \times 10^{10}/\text{cm}^2$ (\blacktriangle) at 520 °C, $2.79 \times 10^{10}/\text{cm}^2$ (\circ), $3.36 \times 10^{10}/\text{cm}^2$ (\square) at 530 °C, and $2.78 \times 10^{10}/\text{cm}^2$ (∇), $2.89 \times 10^{10}/\text{cm}^2$ (\triangle) at 540 °C. In (c) dot densities are $2.55 \times 10^{10}/\text{cm}^2$ (\circ), $2.73 \times 10^{10}/\text{cm}^2$ (\square), $2.78 \times 10^{10}/\text{cm}^2$ (\triangle) at 550 °C. The solid curve is the analytic expression, which is given by $[1 - K_0(r/\xi)/K_0(r_0/\xi)]^2$. Here K_0 is the zeroth-order modified Bessel function, r_0 is the average dot lateral size, and ξ is the average separation $\sim 1/\sqrt{N}$.

For the two-dimensional island, the scaling law for the island separation is also studied.^{15,16} By studying island separation scaling, we can more clearly see how dots nucleate. Therefore, we studied the scaling for the pair distribution function of InAs quantum dots. According to the scaling assumption, the probability of finding another dot separated by distance \mathbf{r} from a particular dot is described by

$$N(\mathbf{r}) = N g\left(\frac{r}{\langle r \rangle}\right). \quad (3)$$

Here N is the whole density of the dots, $\langle r \rangle \sim 1/\sqrt{N}$ is the average distance between dots, and $g(r/\langle r \rangle)$ is the pair distribution scaling function. Figure 4 shows the pair distribution scaling function of InAs quantum dots. We confirmed that the scaling law (3) held at 490 °C and higher growth temperatures. The solid curve is from the analytic solution of rate equations which exclude adatom detachment, and which is practically the same as the homoepitaxy simulation model

with critical cluster size $i=1$. Therefore we conclude that there is no detachment of adatoms in the growth process in the site of the rather high growth temperature. We note that the scaling function has a depletion of dots at small separation. This is because a dot acts as a sink for diffusing In adatoms.

Figure 4(c) shows the pair distribution scaling functions for the sample at 550 °C; the scaling function was quite different from that at lower temperatures. This scaling function has a probability more than 1 at small separation and decays to 1 at $r/\langle r \rangle \approx 3$. Therefore we conclude that a dot did not act as a sink at 550 °C. Rather, dots tend to be formed near other dots.

Both the volume distribution and pair distribution scaling functions agreed well with those of the growth model with critical cluster size $i=1$ from 490 °C to 540 °C. Therefore, we conclude that the dot formation is somehow explained by a surface diffusion model in which a monomer can diffuse but dimers cannot. We must add, however, that this is surprising considering the high growth temperature of 490 °C to 540 °C (In homoepitaxy of Fe on Fe, the model with $i=1$ described the growth at $T < 250^\circ\text{C}$).

IV. CONCLUSION

We have found the volume and pair distribution scaling functions which are not changed by growth temperature from 490 °C to 540 °C. Both scaling functions agreed with those for the homoepitaxy simulation model with critical cluster size $i=1$. Therefore, we conclude that the growth of self-assembled quantum dots can be described by the surface diffusion of In adatoms where only monomers can diffuse and that there is no detachment of a monomer from the island which once formed. The dot volume fluctuation is determined by the stochastic process of the surface diffusion. Therefore, we can explain the dot volume and growth process without considering the effects coming from strain. When we increased the growth temperature to 550 °C, the scaling function was quite different, and we should consider other growth mechanisms.

ACKNOWLEDGMENTS

This work was supported by a Grant-in aid for Scientific Research from the Ministry of Education, Science, Sports and Culture (No. 09450001), and also by the Asahi Glass Foundation.

-
- ¹J. A. Strosio and D. T. Pierce, Phys. Rev. B **49**, 8522 (1994).
²V. Bressler-Hill, S. Varma, A. Lorke, B. Z. Nosho, P. M. Petroff, and W. H. Weinberg, Phys. Rev. Lett. **74**, 3209 (1995).
³A. R. Avery, H. T. Dobbs, D. M. Holmes, B. A. Joyce, and D. D. Vvedensky, Phys. Rev. Lett. **79**, 3938 (1997).
⁴T. R. Ramachandran, R. Heitz, P. Chen, and A. Mudhukar, Appl. Phys. Lett. **70**, 640 (1997).
⁵N. P. Kobayashi, T. R. Ramachandran, P. Chen, and A. Madhukar, Appl. Phys. Lett. **68**, 3299 (1996).
⁶G. S. Bales and D. C. Chrzan, Phys. Rev. B **50**, 6057 (1994).
⁷J. G. Amar, F. Family, and Pui-Man Lam, Phys. Rev. B **50**, 8781 (1994).
⁸C. Ratsch, A. Zangwill, P. Smilauer, and D. D. Vvedensky, Phys. Rev. Lett. **72**, 3194 (1994).
⁹A.-L. Barabási and H. E. Stanley, *Fractal Concepts of Surface*

Growth (Cambridge University Press, Cambridge, England, 1995), p. 178.

- ¹⁰M. C. Bartelt and J. W. Evans, Phys. Rev. B **46**, 12 675 (1992).
¹¹Y. Ebiko, S. Muto, S. Itoh, D. Suzuki, K. Shiramire, and T. Haga, Phys. Rev. Lett. **80**, 2650 (1998).
¹²Y. Chen and J. Washburn, Phys. Rev. Lett. **77**, 4046 (1996).
¹³J. G. Amar and F. Family, Phys. Rev. Lett. **74**, 2066 (1995).
¹⁴J. M. Gérard, J. B. Génin, J. Lefebvre, J. M. Moison, N. Le-bouché, and F. Barthe, J. Cryst. Growth **150**, 351 (1995).
¹⁵M. C. Bartelt and J. W. Evans, Phys. Rev. B **46**, 12 675 (1992).
¹⁶M. C. Bartelt, M. C. Tringides, and J. W. Evans, Phys. Rev. B **47**, 13 891 (1993).
¹⁷D. Leonard, K. Pond, and P. M. Petroff, Phys. Rev. B **50**, 11 687 (1994).